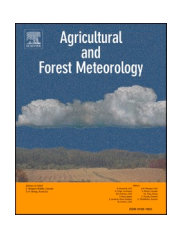
ELSEVIER

Contents lists available at ScienceDirect

Agricultural and Forest Meteorology

journal homepage: www.elsevier.com/locate/agrformet





Analysis of agriculturally relevant rainfall characteristics in a tropical highland region: An agroecosystem perspective

Dereje Ademe ^{a,b,c,*}, Benjamin F. Zaitchik ^b, Kindie Tesfaye ^d, Belay Simane ^e, Getachew Alemayehu ^c, Enyew Adgo ^c

- ^a Debre Markos University, College of Agriculture and Natural Resources, Debre Markos, Ethiopia
- ^b Department of Earth and Planetary Sciences, Johns Hopkins University, Baltimore, MD 21218, USA
- ^c Bahir Dar University, College of Agriculture and Environmental Science, Bahir Dar, Ethiopia
- ^d International Maize and Wheat Improvement Center (CMMYT), Addis Ababa, Ethiopia
- e Addis Ababa University, College of Development Studies (Center for Environment and Development Studies), Addis Ababa, Ethiopia

ARTICLE INFO

Editor: Dr. J Laubach

Keywords:
Agroecosystem
Forecast
Length of growing period
Rainfall cessation date
Rainfall onset date

ABSTRACT

Analysis of Rainfall onset date (OD), cessation date (CD), and length of growing period (LGP) for specific sites in highly dissected topography and highly variable climate may not provide actionable information for crop production planning. In tropical highland regions information on these parameters is scant at a resolution relevant for targeted management. This study examined recent (1981-2016) OD, CD, and LGP variability and trends for the main rainy season in different agroecosystems (AESs) in the northwestern Ethiopian Highlands. Onset criteria were derived from surveys, rainfall data, and previous literature whereas cessation criteria were set from the soil water holding capacity (WHC), daily reference evapotranspiration (ETo), and daily rainfall in each site. Dry spells (DS) were analyzed for the small rainy season in higher elevation AESs where the season is relevant for potato production. All analyses were performed using site specific data grouped by agroecosystem (AES), a unit that has similar climate, soil, crop, and farm management for better agricultural decisions. Results show high inter-annual variability of OD and CD, and LGP exhibited a significant trend in some AES and greater variability in higher elevation AES. Generally, trend analysis results showed early onset and cessation of rainfall. Significant increasing trends and variabilities in DS and OD may significantly affect crop production and thus AES specific crop production calendar should be revised to minimize crop failure. The analysis also confirmed that farmers perception is consistent with meteorological analysis. The results emphasize the importance of AES-based improved seasonal weather forecasts and tailored climate information services to guide farm decisions and improve management of climate variability by smallholder farmers. It also concluded that AES level analysis can better provide actionable information for decision makers and growers than site specific and scattered studies as mosaic results are reported between sites grouped in the same agroecosystem.

1. Introduction

Rainfed crop production has always been vulnerable to precipitation variability. This is particularly true in regions with significant climate variability and low input production systems, which offer farmers few options to compensate for unexpected weather patterns. Both of these conditions apply to the Choke Mountain Watersheds, located in the Blue Nile Highlands of Ethiopia (Fig. 1). Crop production in the area is constrained by many challenges, including fluctuations in rainfall patterns (Urgessa, 2014), emerging trends in prevailing climate conditions

(Ademe et al., 2020; Mellander et al., 2013), and poor understanding of climate variability coupled with low access to tailored climate information (Gbangou et al., 2019). The area is also characterized by significant elevation gradients and dissected topography that lead to significant spatial variability in climate and associated diversity in cropping systems, such that a localized, agriculturally appropriate lens must be applied when considering the impacts that large-scale climate variability and change might have on farming conditions across the region.

For farmers across cropping zones on Choke Mountain, the rainfall

E-mail address: ademe.dereje@gmail.com (D. Ademe).

^{*} Corresponding author.

onset date (OD) and length of growing period (LGP)—which is primarily a function of the period between OD and rainfall cessation date (CD)—are particularly important aspects of climate variability. The importance of these parameters for crop production has long been appreciated on Choke Mountain and in subsistence agricultural systems more broadly (Gbangou et al., 2019; Sarr, 2012). Variability in OD affects planning in input distribution, land preparation, and sowing date determination, while both OD and LGP have significant impacts on crop yields (Eggen et al., 2019; Limantol et al., 2016).

Uncertainty in OD may greatly vary among agroecosystems (AESs) and can lead to suboptimal planting dates, which can in turn lead to crop failure and reduce growing time and crop yields because of dry spell risk and terminal moisture stress, respectively (Akinseye et al., 2016). If farmers plant too early, following false start of rain, they generally need to re-sow or accept much reduced yields because long dry spells (Eggen et al., 2019) during the sensitive early growth stage of crops causes the death of seedlings (Basu et al., 2016), resulting in low plant population and ultimately low yield. In contrast, delay in planting with the fear dry spell following early onset will result in attempts to plant in muddy fields with low soil temperature, which leads to poor seedlings and crop stand (Selvaraju, 2011). Late planting will also reduce LGP, thereby making crops vulnerable to terminal moisture stress that might reduce yield. Thus, timing in OD is the most significant factor that determined the types of crops grown in the area and their productivity (Suryabhagavan, 2017; Viste et al., 2013).

Rainfall cessation date also had effect on crop yield and farm profitability. Early cessation of rain usually resulted in terminal moisture stress and subsequent yield reduction. Contrary to this, extended rainfall will interfere with harvest operations and resulted in crop loss. Though farm decision is not equally affected by OD and CD, some options like crop selection would also be viable if farmers get prior information about rainfall cession date. LGP can also affect the type of crops and varieties to be grown in the area provided that prior information of OD and CD are determined subsequently LGP is estimated. In years where long LGP is expected, late maturing crops and varieties can be used to minimize the effect of rain during harvest. On the other hand, if LGP is

expected to be short for the coming season early maturing crops and varieties will be selected to avoid terminal drought and subsequent yield reduction.

Faced with these impacts, farmers can significantly benefit from prior information about rainfall onset, which can enable them to synchronize planting dates to the predicted OD thereby to improve the feasibility of rainfed agriculture (Amarasingha et al., 2015). In the context of climate change, information on trends and changing variability of OD and CD are vital to design long term strategies like crop choice and other farming calendars (Gbangou et al., 2019).

Despite their critical importance to crop production, statistical information on OD and CD in the study area are scant and only survey and interview information's are available. A survey conducted in 2011 in the study area showed that 90% of the respondents perceived a change in the timing of rains (Amdu et al., 2013). Another survey conducted in the same area also showed that 56%, 74%, and 78% of the respondents perceived early onset, late onset, and early cessation of rainfall, respectively (Weldlul, 2016). Framers also explained that OD is the key determinant factor for farm productivity, both due to its direct impacts and its implications for LGP. They stated that OD is inconsistent, exhibiting high interannual variability. Another interview conducted in the lower part of the watershed revealed that farmers experienced from severe yield reduction to total crop failure due to unpredictable OD and false rainfall start (Eggen et al., 2019). However, all of the data are perceptions and none of these addressed the statistical tests. Moreover, site-specific analysis in a rugged topography may fail to provide actionable information and documenting and implementing site-specific crop production calendar particularly in fragmented and subsistent farming is costly and required many resources and skill. Surveys were also conducted in the watershed without considering climatic, farm management and related discrepancies among AESs. This paper was hence aimed at (i) analyzing the OD, CD, and LGP in various AESs and (ii) analyzing trends of OD, CD and LGP in each AESs located in the Choke Mountain watersheds for the last 36 years (1981-2016) to see whether diffidence in meteorological indices are found among AESs and highlight whether implications of the analysis are different on not for

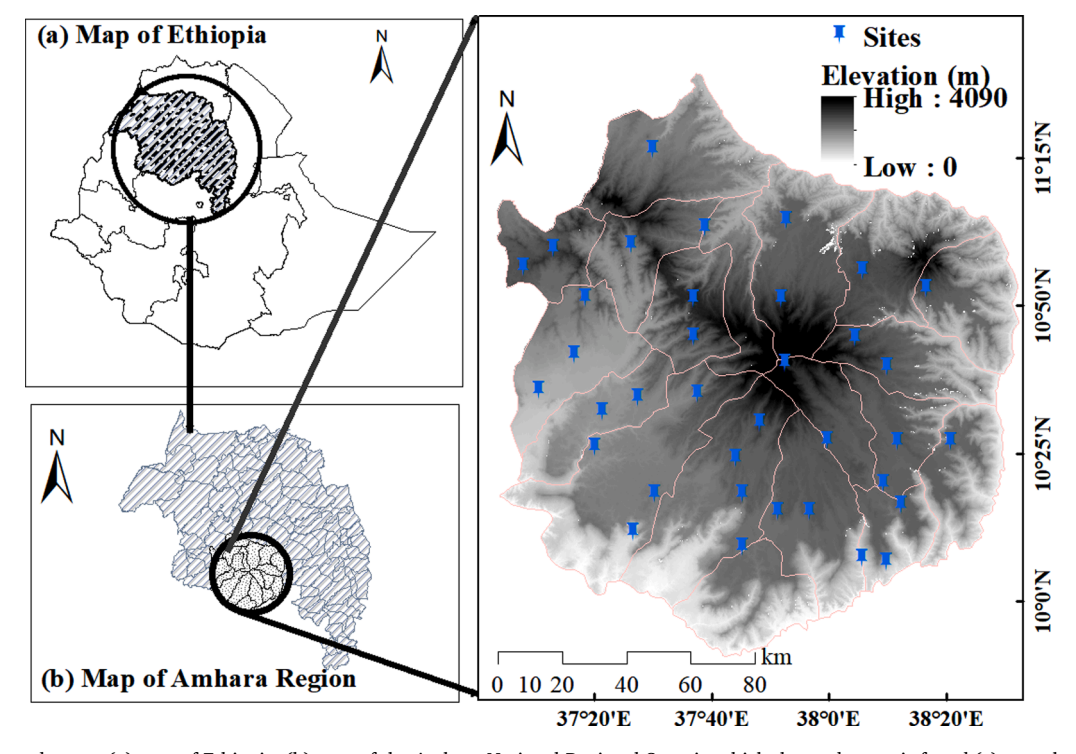


Fig. 1. Map of the study area: (a) map of Ethiopia, (b) map of the Amhara National Regional State in which the study area is found (c) map that shows study area with the topographic information and location of sites.

different AESs.

2. Materials and methods

2.1. Description of the study site

The Choke Mountain watersheds are situated in the Blue Nile Highlands of Ethiopia, in the northwest of the country $(9^{\circ}45'-11^{\circ}30' \text{ N}; 37^{\circ}5'-38^{\circ}20' \text{ E})$ and have elevation ranging from 800 to 4200 masl (Fig. 1).

The area experiences intense land pressure due to an increasing population and agriculture-based economy, which is entirely dependent on smallholder low-input-output agriculture. This land pressure has led to significant changes in land use, including loss of previously forested areas (Aramde, 2014; Gessesse and Melesse, 2018; Teferi et al., 2010). Farming is predominantly a crop-livestock mixed system that is operated by independent farmers on small plots (Simane et al., 2013, 2012; Zaitchik et al., 2012). Nitisols, Vertisols, Andosols, and Acrisols (Zaitchik et al., 2012) are dominant soil types of the area. Dry valleys, gently rolling, deep soil midland plains, and cool wet alpine zones are found within a short distance of the mountain, and complex topography leads to strong local contrasts in precipitation and temperature (Simane et al., 2012; Zaitchik et al., 2012).

Three distinct seasons are found in the study area: small rain season (Feb–May), main rain season (Jun – Sep), and dry season (Oct – Jan). The two rainy seasons in the region; the small *belg* rains in spring and the main *kiremt* rains in summer, have significant implications for agriculture. The dry season is also important, as extended rain in the dry season can interfere with harvest operations and result in the loss of produce (Asfaw et al., 2018; Polsky and von Keyserlingk, 2017).

Seasonal precipitation in the area is highly correlated with the movement of inter-tropical convergence zone with most rain falling in *Kiremt* season. The distribution of rainfall in the area exhibits strong local variability associated with topographic gradients. Precipitation is highly convective, characterized by short intense erosive bursts (Zaitchik et al., 2012). Interannual precipitation variability is significant (Ademe et al., 2020; Zaitchik et al., 2012) and has major impacts on agricultural production and soil erosion. El Nino Southern Oscillation (ENSO), Indian ocean SST, and the Atlantic Pasfic Decadal Oscillation as reported to be the causes of such precipitation variability (Zaitchik et al., 2012)

Typically the prevailing climate of the study region is tropical highland monsoon, however, the topographic gradient yields climate zones that range from warm to cool, resulting in cropping systems that allow to grow crops of both tropical and temperate origins. This diversity is highly relevant when considering agricultural impacts of climate variability and change. Temperate origin crops at higher elevations benefit from or are entirely dependent on seasonally cold temperatures, for example, while crops at low elevations are grown in hot environments subject to significant water stress. To account for this diversity, we apply the agroecosystem (AES) as an agriculturally relevant unit of aggregation. The AES represents the intersection of a common set of climate conditions, soil properties, and farming systems, and thus offers a unit that is relevant for analyzing and communicating impacts of climate on agriculture (Simane et al., 2013). A brief description of the AES in the mountain watersheds is presented in Table 1.

2.2. Research approach

2.2.1. Data type and source

Precipitation records for 36 sites of interest were extracted from the Enhancing National Climate Services (ENACTS) dataset, through request to the Ethiopian National Meteorological Agency (NMA). ENACTS is a 4×4 km gridded data reconstructed from weather stations and meteorological satellite records from 1981 to 2016. The ENACTS

Table 1Characteristics of Agroecosystems of the Choke Mountain Watersheds (adapted from Simane et al., 2013).

Agroecosystem	Farming system	Traditional Climatic Zone*	Dominant soils	Major crops
AES1: Lowlands and Abay valley	Fragmented sorghum- based extensive	Upper Kola	Leptosols Cambisols	Sorghum, tef, maize, haricot bean
AES2: Midland plains with black soil	Intensive teff- based	Lower Weyna Dega	Vertisols	Teff, durum wheat, barley, chickpea, grass pea
AES3: Midland plains with brown soil	Intensive maize-wheat based	Lower Weyna Dega	Nitosols Alfisols	Wheat, maize, tef
AES4: Midland sloping lands	Semi- intensive wheat/barley based	Upper Weyna Dega - Lower Dega	Leptosols Nitosols Alfisols	Wheat, tef, barley, Engido (Avena spp.)
AES5: Hilly and mountainous highlands	Potato/barley based	Upper Dega	Leptosols Andosols	Potato, barley, faba bean, Engido

 $[\]ensuremath{^{^{\circ}}}$ Kolla, Woyna Dega and Dega refers to Lowland, Midland and Highland, respectively.

product makes use of an extensive set of NMA station records, merged with a locally calibrated version of the Tropical Applications of Meteorology Using Satellite Data and Ground-Based Observations (TAMSAT) satellite rainfall estimates (Dinku et al., 2016, 2014). The resulting data product shows good performance across the country, and is highly correlated with the station data (Alemayehu and Bewket, 2017; Dinku et al., 2016, 2014). Details about the ENACTS data construction are available in Dinku et al. (2016, 2014) and IRI (2016).

Daily reference evapotranspiration data for each site were estimated from downscaled Modern-Era Retrospective analysis for Research and Applications, Version 2 (MERRA-2) temperature estimates (Gelaro et al., 2017) and Climate Hazards Group InfraRed Precipitation with Station data (CHIRPS) precipitation estimates (Funk et al., 2015) following Hargraves method (Aguilar et al., 2011), which is appropriate for dry season reference evapotranspiration estimates (Gotardo et al., 2016). In-depth interview and focus group discussion were conducted to define criteria for the start of rain onset date and the possible planting dates using unstructured questionnaires in December 2016 and January 2017.

2.2.2. Data preparation and quality control

Homogeneity and change points were checked using the penalized maximal F test (Wang, 2008a, 2008b). Precipitation and reference evapotranspiration data were arranged as per the data format requirements of INSTAT 3.37+ statistical software.

2.2.3. Data analysis

2.2.3.1. Rainfall onset analysis. A focus group discussion was held with farmers to understand when and at what condition they define a sowing date. In all agroecosystems, farmers explained that at least three consecutive days "adequate rain" that can sufficiently moisten the soil should fall to start planting. We refer to this as the "farmers' definition" of OD. Then the Stern method (Stern et al., 1981) that stated the onset of rain was considered when 20 mm of accumulated rainfall in a day or two was modified to satisfy the farmers' definition. Thus, rain onset was defined as the first rain day of at least three consecutive rain days resulting in a total rain of 20 mm or more (Mellander et al., 2013). Farmers further explained that they frequently experience crop failure due to breaks in rain some days after the start of the rain—that is, the

perceived OD was a "false start" to the cropping season. Thus, an additional caveat was added to avoid any dry spell risk by requiring that no period of nine (Sorghum) (Assefa et al., 2010) and seven (Maize) (Brewbaker, 2003) or more consecutive dry days occur in the 30 days following a potential OD diagnosis. We refer to this conditioned Stern method definition of the onset date as the "optimal definition". These crops are planted in April to early May. The earliest possible rain onset day was determined as 1-15 April (April 1 for AES4 and AES5, and April 15 for AES1-AES3) based on information obtained from focus group discussion and in-depth interviews with farmers in each agroecosystem (Supplementary Table 1).

2.2.3.2. Rainfall cessation analysis. The rain cessation date was defined as any date after September 5 when the soil water balance goes to zero. To determine the soil water balance, the water holding capacity of the soil was estimated based on the soil type of each site. A soil sample was taken from 74 farm plots in all agroecosystems and soil texture and soil organic matter was determined in the Debre Markos soil laboratory. Percent gravel in each field was determined based on expert judgment at the field during sample collection. Then, the soil water holding capacity of the fields was estimated using the soil water characteristics (SWC) model developed by USDA (Saxton et al., 1986). Results summarized by Agroecosystems are presented in Table 2.

Then for each of the 36 locations and for each of the 36 years in the analysis period, the daily rainfall and reference evapotranspiration data were recorded and the available soil water was simulated with the water balance module in the INSTAT 3.37+ software (Stern et al., 2006). The resulting estimates of rain onset and cessation dates based on the water balance module output are presented in Supplementary Fig. 1.

The analysis is performed for each site independently (without any averaging across sites), and the resulting results are then averaged and summarized at AES level. Probabilities of exceedance of the rain onset and cessation dates, and the length of the growing season, were calculated using the frequency analysis module in INSTAT 3.37+ software (Stern et al., 2006). This is done by ranking the data values in descending order and assigning a serial rank number to each value to obtain a plotting position which corresponds with the frequency of exceedance on a probability plot. After selecting the distribution assumption, data values were plotted, and a theoretical distribution line drawn. The 80, 50 and 20% probabilities of exceedance were determined and used as indicators of early, normal, and late onset and cessation dates, respectively. For the length of growing season analysis, the 80, 50 and 20% probabilities of exceedance were determined and used as indicators of a short, normal, and long season, respectively. The data were fitted with normal distribution.

2.2.3.3. Dry spell analysis. A dry spell of duration "d" is defined as a period of "n" consecutive dry days (Ratan and Venugopal, 2013). The maximum dry spell length for the small rain season months (February–May) was analyzed using the same software for AES₄ and AES₅, because this season is important in these agroecosystems for planting of potato.

Table 2Soil physical properties, dominant soils and water holding capacity (WHC) in the Choke Mountain Watersheds.

AES	Clay (%)	Sand (%)	Gravel (%)	OM (%)	Dominant soils*	WHC (mm/m)
1	54	18	15-50	2.65	Leptosols	60 – 100
2	67	8	0	2.48	Vertisols	150
3	57	13	0	3.44	Nitisols	110
4	61	14	15	2.27	Nitisols	100
5	52	16	5	3.53	Andosols	120

^{*} Simane et al. (2013).

2.2.3.4. Correlation analysis. Correlations reported in this study were all calculated using a standard Pearson correlation coefficient. In addition to looking at correlation between meteorological parameters, we calculate correlations between meteorological indices and geographic features (latitude, longitude, altitude, slope, and aspect), making use of a 12 meter resolution digital elevation model (DEM) obtained from satellite data.

2.2.3.5. Trend analysis. Trend of rainfall onset date, cessation date, growing season length and dry spell length was analyzed using the Mann-Kendall trend test and Sen's slope estimator (Mann, 1945; Sen, 1968) as implemented in R-package *Rclimdex 1.0* (Karl et al., 1999).

The Mann-Kendall test was applied using the formula (Eq. (1)):

$$S = \sum_{k=1}^{n-1} \sum_{i=k+1}^{n} sgn(x_i - x_k)$$
 (1)

where n= number of data points, x_k and x_j = data values in time series k and j (j>k), $sgn(x_i-x_k) = sign$ function as (Eq. (2)):

$$sgn(x_{j} - x_{k}) = \begin{cases} 1 & \text{if } x_{j} - x_{k} > 0 \\ 0 & \text{if } x_{j} - x_{k} = 0 \\ -1 & \text{if } x_{j} - x_{k} < 0 \end{cases}$$
 (2)

The variance of S is computed as (Eq. (3)):

$$VAR(S) = \frac{\left[n(n-1)(2n+5) - \sum_{p=1}^{q} t_p (t_p - 1)(2t_p + 5)\right]}{18}$$
(3)

Where q=number of tied groups and t_p = the number of data points in the p^{th} group.

The values of *S* and *VAR(S)* were used to compute the test statistic Z_s as follows (Eq. (4)):

$$Z_{s} = \begin{cases} \frac{S-1}{\sqrt{VAR(S)}} & \text{if } S > 0\\ 0 & \text{if } S = 0\\ \frac{S+1}{\sqrt{VAR(S)}} & \text{if } S < 0 \end{cases}$$

$$\tag{4}$$

Positive/negative Z indicates an upward/downward trend for the period.

Sen's slope estimator (Sen, 1968) was used to estimate the slope of the trend. Sen's method can be used in cases where the trend can be assumed to be linear and is equal to (Eq. (5)):

$$f(t) = Q_t + B \tag{5}$$

Where f(t) is a continuous monotonic increasing or decreasing function of time, Q_t is the slope and B is a constant. The slopes of all data value pairs were calculated to get the slope estimate Q as (Eq. (6)):

$$Q_i = \frac{x_j - x_k}{i - k} \text{ for } i = 1, \dots, N,$$
 (6)

Where X_j and X_k are the data values at times j and k (j>k). Hence we only have one datum in each period, and N is computed as (Eq. (7)):

$$N = \frac{n(n-1)}{2} \tag{7}$$

where n is the number of time periods. The N values of Q_i were ranked from smallest to largest and the median of slope or Sen's estimator was computed as (Eq. (8)) (Gocic and Trajkovic, 2013):

$$Q_{med} = \left\{ Q_{\left[\frac{N+1}{2}\right]} \right\} + Q_{\left[\frac{N+2}{2}\right]}$$

$$\frac{2}{2} \quad \text{if N is even}$$
(8)

Positive/negative values of Qi indicate an increasing/decreasing trend, respectively. Confidence intervals (C_{α}) about the time slopes were used to test significance of the trend and were computed as follows (Eq. (9)) (Gilbert, 1987):

$$C_a = z_{1-\alpha/2} \sqrt{Var(S)} \tag{9}$$

Where Var(S) is defined in Eq. (3) and $z_{1-\alpha/2}$ is obtained from the standard normal distribution table.

2.2.3.6. Spatial interpolation. Median onset and cessation dates and length of growing period, their trends, and probability levels at land-scape level are interpolated from site values. Inverse distance weighting (IDW), Ordinary Kriging (OK), and Spline interpolation methods were applied and their interpolation performance was evaluated using Mean absolute error (MAE), Root Mean Square Errors (RMSE) and the Index of Agreement (D) statistics. IDW was found to perform best (Supplementary Table 2). IDW is also a commonly used approach for estimation of missing data in hydrology and geographical sciences (Teegavarapu and Chandramouli, 2005). It was implemented in this study using ArcMap 10.6.1. The IDW interpolated values were computed as (Eq. (10)):

$$\theta_m = \frac{\sum_{i=1}^{n} \theta_i d_{mi}^{-k}}{\sum_{i=1}^{n} d_{mi}^{-k}} \tag{10}$$

Where θ_m is the observation at the location m; n is the number of stations; θ_i is the observation at station i, d_{mi} is the distance from the location of station i to location m; and k is referred to as friction distance, and is fixed at 2.0 in this study.

3. Results

3.1. Summary of site level rainfall onset date, cessation date and length of growing season

3.1.1. Rainfall onset

Site level rainfall onset and cessation dates and growing season length analysis showed that the west and southwest part of the mountain exhibit earlier median onset of rain (Fig. 2a). In some areas of the western part of the study area, the rain started as late as May 16 – May 27. In most areas of the western part of the study area (including all sites in AES $_3$, some sites in AES $_4$ and AES $_5$), the rainfall onsets occurred between May 28 – June 7. The rainfall onset date in northern, central, and southeastern parts of the mountain have a rain onset between June 8

– June 18. Late onset of rain is observed in the northeastern and eastern part of the study region, including most sites in AES_2 and some sites in AES_1 (June 19 -June 29).

3.1.2. Rainfall cessation

Rainfall cessation date had a different spatial pattern than rainfall onset date. Early cessation (Oct 3 – Oct. 14) of rain occurred in few sites of AES $_1$ followed by several sites of in southwestern, southern, southeastern parts in AES $_2$ and AES $_1$ and some pocket sites in AES $_5$ where rainfall cessation occurred between Oct. 15 and Oct. 25 (Fig. 2b). Most sites found in all AES except AES1 have rainfall cessation date between Oct. 26 – Nov. 05. In the northeastern and northwestern parts of the watershed the rain ceased between Nov. 06 – Nov. 16 (Fig. 2b).

3.1.3. Length of growing season

Average growing season length also showed a well-defined spatial pattern, with a few exceptions. The shortest growing season length ranged from 110–127 days and occurred in the eastern and southeastern parts of the study region (in AES $_1$ and parts of AES $_2$) and in a few sites of AES $_5$ and AES $_4$ (Fig. 2c). Most areas in the watershed (including most areas of AES $_3$ and many areas of AES $_4$) have a growing season length ranging from 128–144 days. Some areas in the northwestern part (AES $_5$) and central part of the watershed have a growing season length between 145–161 days, and only a few sites in the western part (AES $_5$) have a growing season length from 162–178 days.

3.2. Agroecosystem level rainfall onset, rainfall cessation and length of growing season

3.2.1. Rainfall onset

At AES level, the median rain onset in the area occurred between June 3–June 18, and AES_1 , AES_3 and AES_5 have a rainfall onset at the mid of the first week of June, while in AES_4 and AES_2 rain started in the second and third week of June, respectively (Table 3).

The longest (84 days) and the shortest (49 days) variation in rain onset date were found in AES_4 and AES_1 , respectively. Interannual variability, explained by the coefficient of variation, in onset date was also high in all agroecosystems, with relatively higher variability in high altitude AES.

The calculated early, normal, and late onset dates of rain in each AES are presented in Fig. 3. AES₁, AES₃, and AES₅ had the same median (50% probability of exceedance) onset date (Jun 04) followed by AES₄ (June 09) and AES₂ (June 18). The 20% probability of onset (indicator of early

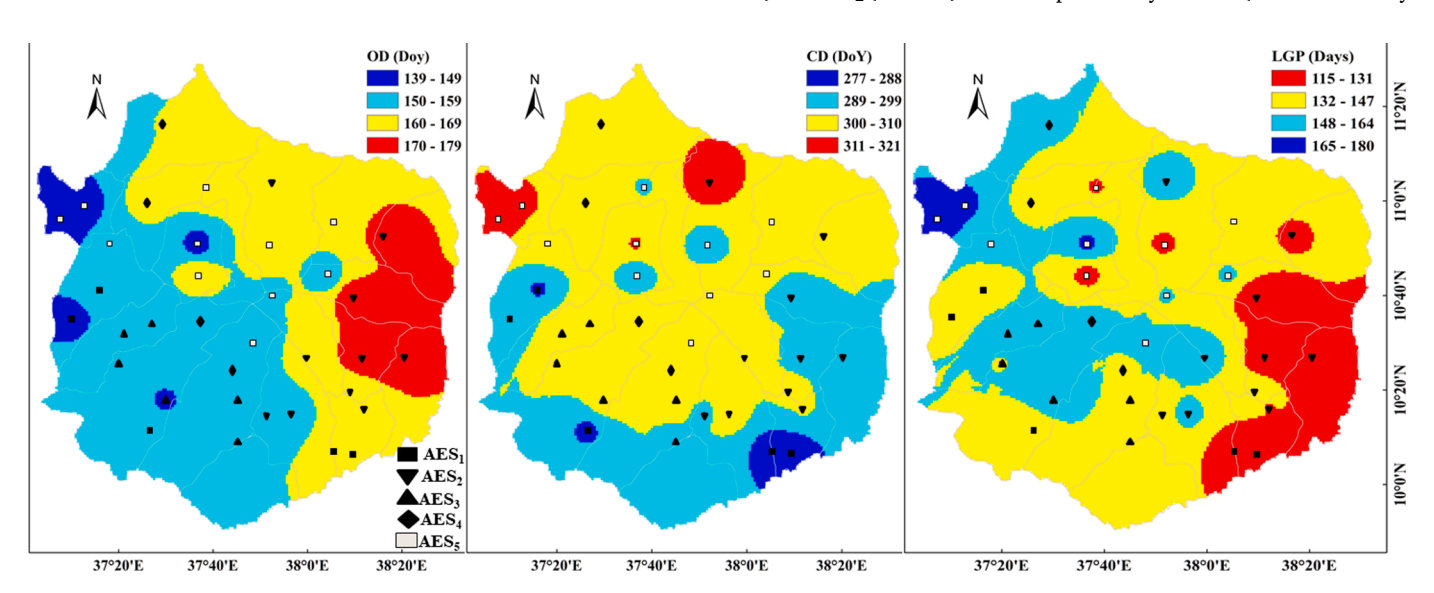


Fig. 2. Median rainfall onset and cessation dates and length of growing period in the Choke Mountain Watersheds (1981-2016). Colors of markers indicate the agroecosystem in which each site is located.

Table 3 Summary of rain onset date in the Choke Mountain Watersheds (1981–2016).

Statistics	AES ₁	AES ₂	AES ₃	AES ₄	AES ₅
Median onset date	04-Jun	18-Jun	03-Jun	09-Jun	04-Jun
Earliest onset date	09-May	20-May	02-May	29-Apr	30-Apr
Latest onset date	26-Jun	25-Jul	08-Jul	23-Jul	18-Jul
Range (days)	49	66	67	84	79
Standard deviation (days)	15	14	17	19	18

AES = agroecosystem.

onset date) came earliest in AES5, followed by AES $_3$, AES $_1$, AES $_4$, and, finally, AES $_2$. The 80% probability of onset (indicator of late onset date) was similar for AES $_1$, AES $_3$, and AES $_5$, and came later in AES $_4$ and AES $_2$. Overall, AES $_2$ onset date is shifted later relative to the other AES across the probability distribution.

Based on second order stochastic dominance analysis, the rainfall generally started earlier in AES_3 than other AESs followed by AES_1 , while AES_2 showed the late onset of rain in 90% of the years (Fig. 3). A ttest also showed that only AES_2 had an onset date that was significantly different from other AES, and the remaining AESs showed statistically insignificant differences in onset date (Supplementary Table 4).

3.2.2. Risk of dry spells

Rainfall onset risk analysis revealed that 56%, 81%, 36%, 83%, and 75% of the years of the study period showed a false start of rain from $AES_1 - AES_5$, respectively, with a discrepancy between the false start and the actual start that could be up to ten weeks long (Supplementary

Fig. 2). This would have negative implications for agricultural practices, as it triggers planting too early and affects all subsequent farm operations. The fact that a false start can cause planting to occur many weeks before the actual objective start of the rainy season brings challenges for farmers on crop and variety choice, and farm operations.

It is also found that 33–78%, 28–64%, 8–33%, and 0–11% of the years showed variations of more than 10, 20, 30 and 60 days between the "optimal onset date" (i.e., the conditioned Stern method definition) and the onset determined by farmers' definition, respectively (Table 4). The analysis revealed that risk of dry spell is very common in all AESs and more pronounced in the higher altitude AESs.

As noted in the introduction, high altitude AES (AES_4 and AES_5) farmers practice potato cultivation during the small rain season. For these farmers, the success of potato production is sensitive to dry spell length during this season. Thus, we analyzed the percentage of one-week, two-week, three-week, and four and above week dry spell

Table 4Percentage of years with rain onset date variations between farmers' definition and statistical analysis.

Difference (days)	Agroecosystems							
	AES ₁	AES_2	AES_3	AES ₄	AES ₅			
≥ 10	53	78	33	75	75			
≥ 20	28	53	28	64	44			
≥ 30	8	33	14	42	31			
≥ 60	0	3	0	11	6			

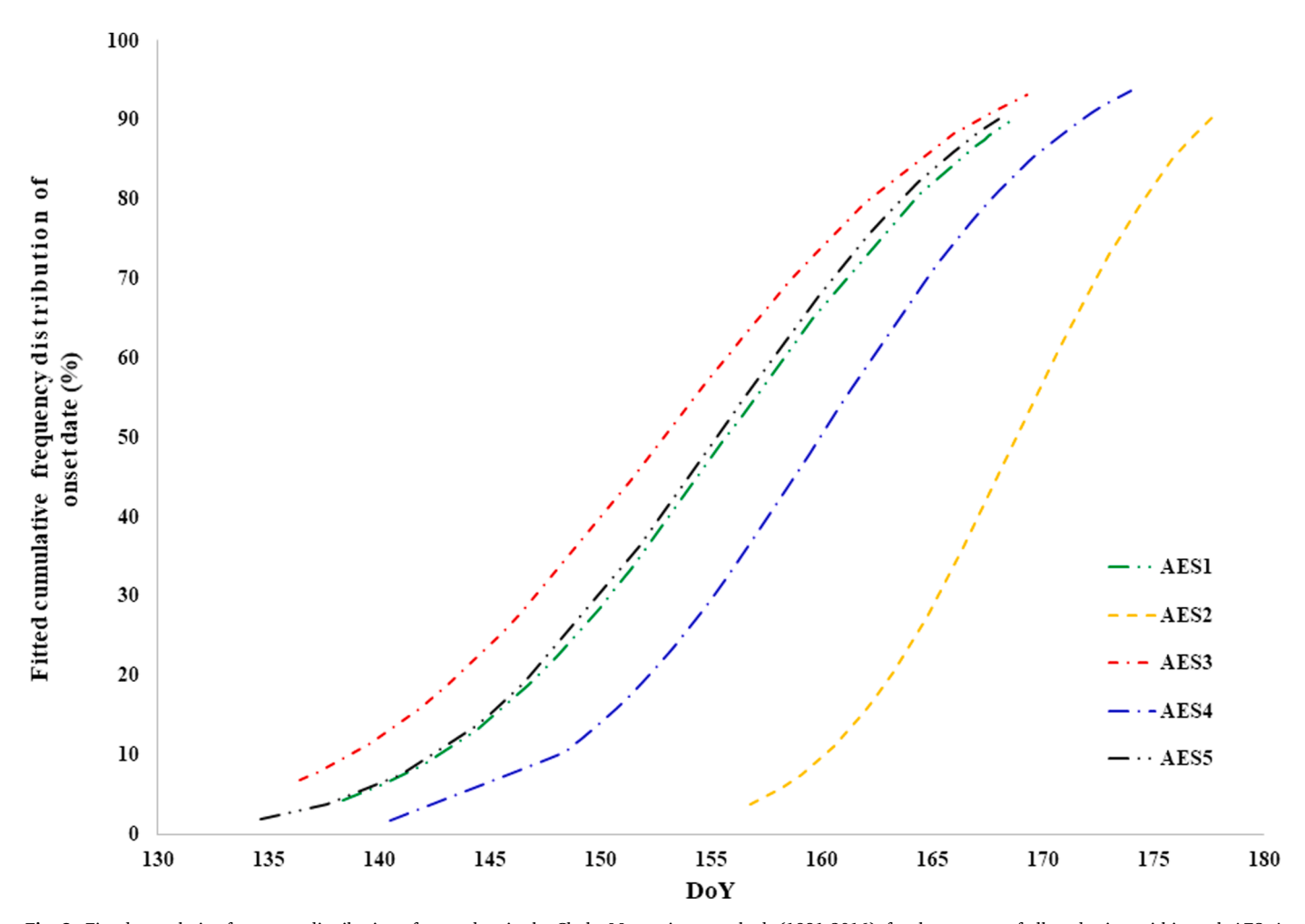


Fig. 3. Fitted cumulative frequency distribution of onset date in the Choke Mountain watersheds (1981-2016), for the average of all study sites within each AES. A normal distribution was fitted for the range of 20 to 80% of the total.

length for potato planting performed at the beginning of each month grouped in the small rain season. Results of dry spell analysis for the small rain season months revealed more than 80% the years experienced more than 28 days (four weeks) dry spell period if planting is done at the beginning of February and or the beginning of March (Fig. 4).

The risk of a > 4 week dry spell is considerably reduced if planting is delayed until the beginning of April, but substantial risk remains: nearly 70% of the years experienced more than two weeks dry spell length and 45 – 65% and 25 – 55% of the years experienced three- and four-weeks dry spell length, respectively, for an April 1 planting date (Fig.4). Planting at the beginning of May also showed a high chance of the occurrence of more than one (78–98%), two (41–61%), and three (17–42%) weeks dry spell length, though the chance of more than four weeks (3–25%) dry spell length was much lower.

Dry spell period for the small rain season also showed high interannual variability. The coefficient of variation of dry spell was 39% and 36%, 53% and 49%, 81% and 79%, and 81% and 45% in February, March, April, and May in AES4 and AES5, respectively (Supplementary Table 5). A trend test for dry spell length also showed a significant increasing trend in February, March, and April in both AES4 and AES5 (Table 5). In AES4, the dry spell length in February, March and April increased by 0.94, 1.15, and 0.37 days per year, respectively. In AES5, the dry spell length in February, March, and April increased by 0.88, 1.44, and 0.25 days per year, respectively (Table 5). However, there is no significant trend in dry spell duration in May.

Table 5Trends of dry spells in dry season months (FMAM) in the Choke Mountain Watersheds (1981–2016).

AES	Feb		March	March		April		May	
	ZMK	Slope	ZMK	Slope	ZMK	Slope	ZMK	Slope	
4	2.15	0.94	2.24	1.15	1.76	0.37	-0.76	-0.08	
5	1.75	0.88	2.60	1.44	1.71	0.25	-1.12	0.10	

AES = Agroecosystems; Z = Mann-Kendall Z test; S= Sen slope; bold values indicated significant trend change. FMAM= February, March, April, and May.

3.2.3. Rainfall cessation

Agroecosystem level median rainfall cessation date in the area falls between 9–30 October. AES_1 had a rain cessation at the beginning of the second week of October, while in the remaining AESs rain ceased between 27–30 October (Table 6). The longest (66 days) and the shortest (41 days) variation in rain cessation date were found in AES $_2$ and AES $_3$, respectively. However, interannual variability, explained by the coefficient of variation, in cessation date was uniform in all agroecosystems.

The calculated early, normal, and late rain cessation date ranges from Oct. 1 – Oct. 22, Oct. 9 – Oct. 30, and Oct. 15 – Nov. 12, respectively (Table 6). AES_1 and AES_4 showed early (Oct. 1) and late (Oct. 22) 80% probability of exceedance, respectively (Fig. 5 and Table 6). However, AES_2 , AES_3 , and AES_5 almost had the same early (80% probability of exceedance) rain cessation dates.

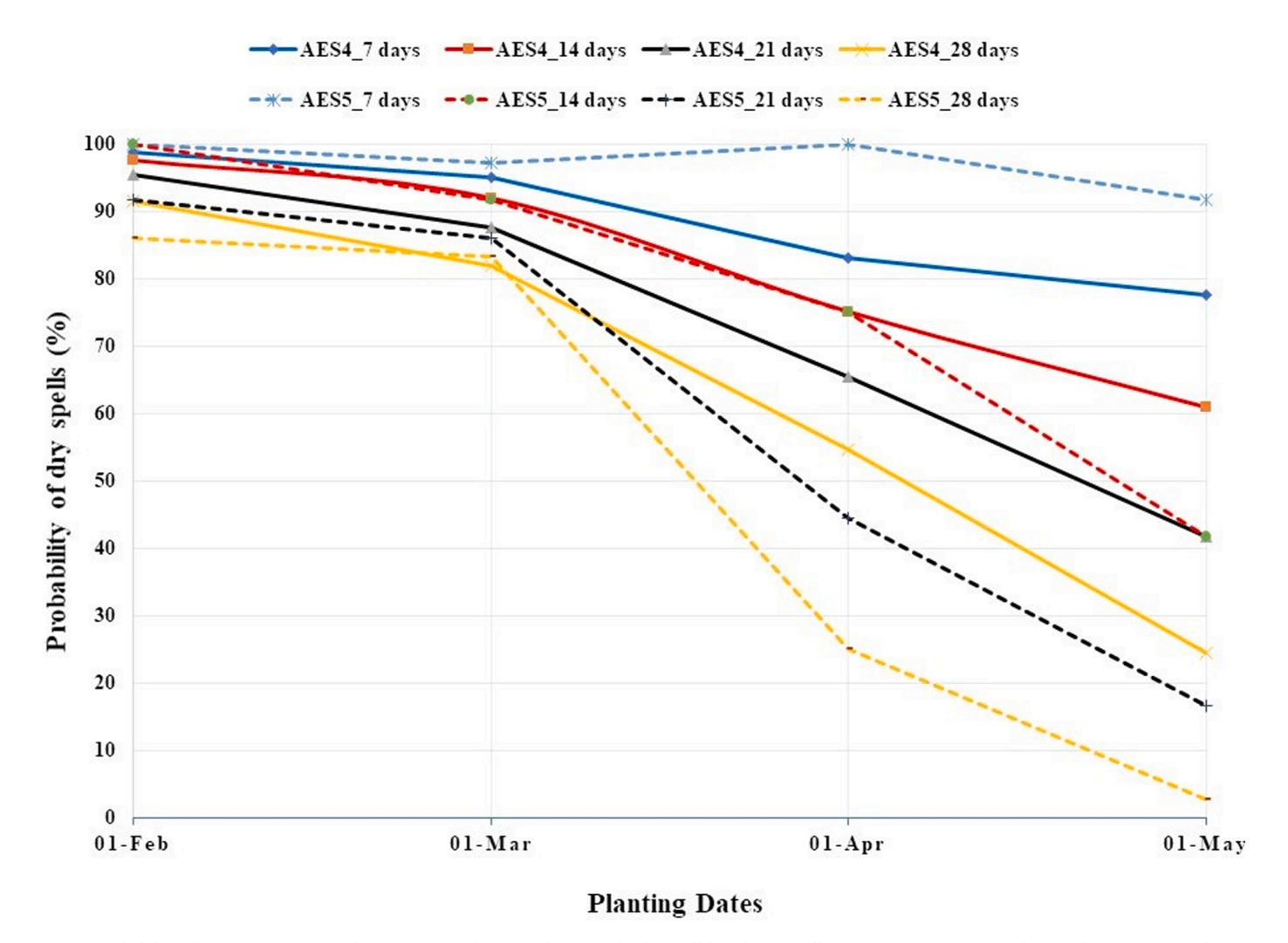


Fig. 4. Probability of percentage of more than one-, two-, three-, and four-weeks dry spell length for small rain season in for FMAM planting dates in AES₄ and AES₅ of the Choke Mountain Watersheds (1981-2016) (FMAM=February-March-April-May, respectively).

Table 6Summary of rainfall cessation date in the Choke Mountain Watersheds (1981–2016).

Statistics	AES_1	AES_2	AES_3	AES ₄	AES ₅
Median cessation date	09-Oct	30-Oct	27-Oct	30-Oct	28-Oct
Earliest cessation date	21-Sep	06-Oct	13-Oct	13-Oct	13-Oct
Latest cessation date	02-Nov	21-Nov	23-Nov	06-Dec	26-Nov
Range (days)	42	66	41	54	45
Standard deviation (days)	8	11	10	12	11

The normal rain cessation date in AES $_1$ took place on Oct 9, while in all other AESs it took place on the 29^{th} and 30^{th} of October (Fig. 5 and Table 6). Similarly, AES $_1$ had the earlier late cessation (20% probability of exceedance) date (Oct. 15) followed by AES $_3$ (Nov. 05), and AES $_4$ had the longest late cessation date (Nov. 12). A large variation in rain cessation date (> 8 weeks) was found in AES $_2$ followed by AES $_4$ (7 weeks), whereas AES $_1$, AES $_3$ and AES $_5$ had about seven weeks variation in cessation date. Generally, the rainfall ceased earlier in AES $_1$, followed by AES $_2$, and other AESs had a similar pattern in rainfall cessation date (Fig. 5). A t-test also showed that the AES $_1$ cessation date was significantly different from the other AESs (Supplementary Table 4).

3.2.4. Length of growing period

Agroecosystem level median growing season length in the area falls between 125-152 days. AES_1 had a shortest growing season, length followed by AES_2 . AES_3 had the longest growing season length followed by AES_5 (Table 7).

The short, normal, and long growing season length in the area occurred between 114–129, 125–152, and 144–169 days, respectively, and the shorter growing season length in each category was found in AES_1 followed by AES_2 (Fig. 6).

The longest variation in growing season length was found in AES₄ (102 days) followed by AES₅ (78 days), while the shortest variation in growing season length of 61, 66 and 68 days was found in AES₁, AES₂ and AES₃, respectively (Table 7). A t-test also showed that only AES₁ and 2 had a significant and shorter LGP and the remaining AESs showed statistically insignificant difference in LGP (Supplementary Table 4).

3.3. Correlation analysis

Correlation analysis between events was also done in each AES (Supplementary Table 6) and the result revealed that onset date and cessation date showed a non-significant weak correlation in each AES. On the other hand, onset date and growing season length showed a

Table 7
Summary of the growing season length in the Choke Mountain Watersheds (1981–2016).

Statistics	AES_1	AES_2	AES_3	AES ₄	AES ₅
Median growing season length (days)	125	132	152	144	149
Range (days)	61	72	68	102	78
Standard deviation (days)	15	16	20	22	19
Coefficient of variations (%)	12	12	13	15	13

AES = Agroecosystem

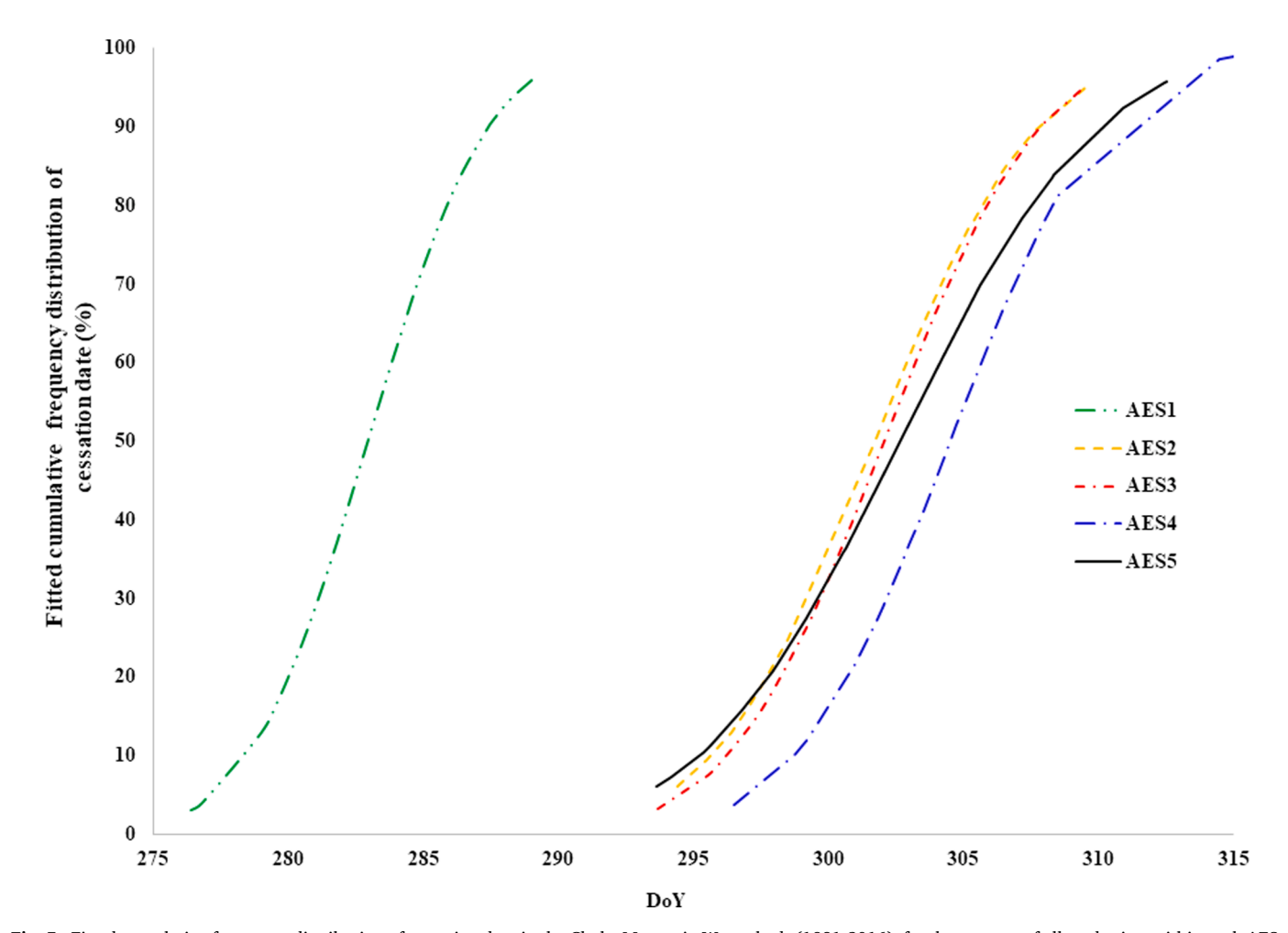


Fig. 5. Fitted cumulative frequency distribution of cessation date in the Choke Mountain Watersheds (1981-2016), for the average of all study sites within each AES. A normal distribution was fitted for the range of 20 to 80% of the total.

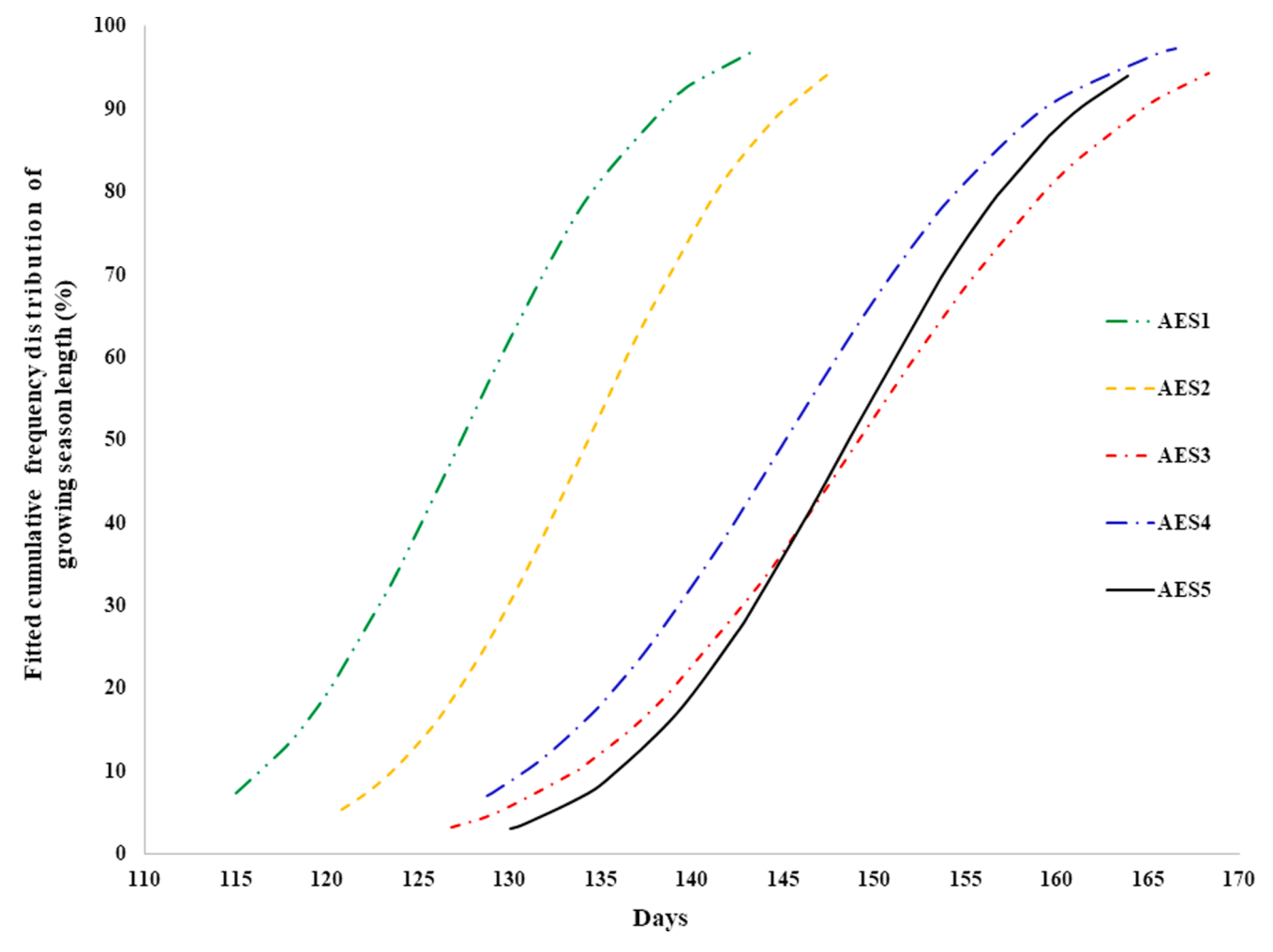


Fig. 6. Fitted cumulative frequency distribution of growing season length in the Choke Mountain Watersheds (1981-2016), for the average of all study sites within each AES. A normal distribution was fitted for the range of 20 to 80% of the total.

significant and strongly negative correlation in each AES (r=-0.74-0.87, p<0.001), which indicated that the early onset of rain contributed to the longer growing season length. Rainfall cessation date and growing season length also showed a significant and moderate correlation in each AES (r=0.31-0.53, p<0.01-p<0.001). Thus, late cessation of rain accounted for longer growing season length. The correlation between onset date and cessation date was insignificant for all sites, suggesting that different large scale climate drivers may be involved early vs. late in the rainy season (Berhane et al., 2014). LGP showed a highly significant and negative strong ($r=-0.79^{***}$) correlation and a highly significant and strong positively strong ($r=0.79^{***}$) correlation with onset date and cessation date respectively, indicating that both onset and cessation dates play an important role in determining LGP (Supplementary Table 7).

Correlation analysis between topographic features and meteorological indices also revealed that none of the topographic features showed a significant correlation with rain onset date (Supplementary Table 7). Cessation date (r=0.49, p<0.01) and length of growing period (r=0.29, p<0.05) showed a significant and weak positive correlation with elevation implying that high altitude areas exhibited a late rain onset date and relatively longer growing season compared to the lowland areas (Supplementary Table 7).

3.4. Trends of rainfall onset date, cessation date and length of growing period at site level

3.4.1. Trends of rainfall onset date

Trend analysis on rain onset date confirmed that 31% of the areas (most of them were found in AES_5) showed a significant decreasing trend (Fig. 7 and Supplementary Table 3).

Some areas in the southwest and west part of the watershed had an earlier onset date (6–11 days earlier per decade). Most areas of the watershed showed early rain onset date that ranged between 0-5 days earlier per decade, while a few areas in southeast and northwest part showed a late rain onset date which lags up to 4 days per decade.

3.4.2. Trends of rainfall cessation date

Trend analysis on rainfall cessation date confirmed that 25% of the areas in the northwestern, central, and southeastern parts of the watershed (most of them were found in AES $_2$, AES $_4$ and AES $_5$) showed a significant decreasing trend (Fig. 7 and Supplementary Table 3). The rain cessation date in these areas decreased by 3–6 days per decade. Most areas of the watersheds showed an earlier rain cessation date trend that ranged between 0–2 days per decade. A few sites in the west, northeast and southern parts of the study area showed a trend towards later cessation date of up to 5 days per decade.

3.4.3. Trends of length of growing period

Trend analysis on growing season length confirmed that 17% of the areas in the western, southwestern, central, northwestern, and

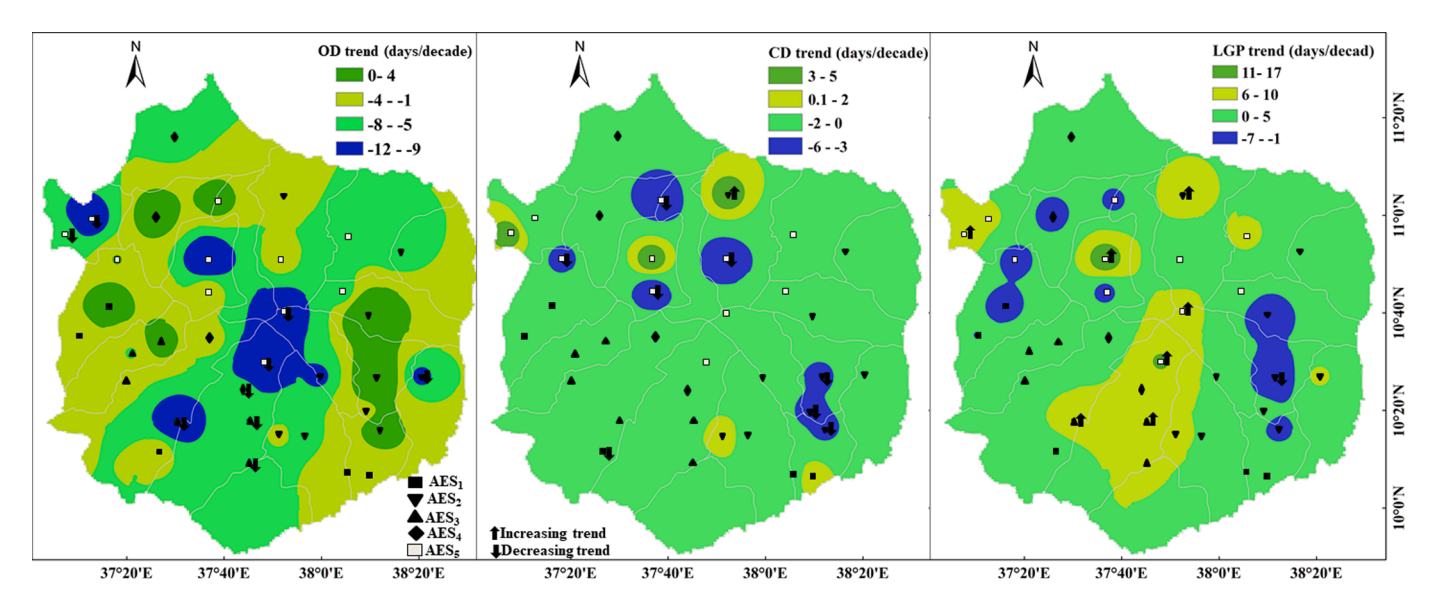


Fig. 7. Trends of rainfall onset and cessation dates and length of growing period in the Choke Mountain Watersheds (1981-2016). Colors of markers indicate the agroecosystem in which each site is located.

southeastern parts of the watershed showed a significant decreasing trend (Fig. 7 and Supplementary Table 3). The growing season length in these areas decreased by seven days per decade. Most sites in the study area showed an increase in growing season length between 1–5 days per decade with insignificant trend. Only 6% of the areas in the watershed showed a significant increasing trend, while a few sites in the west, northeast and southern parts of the study area showed an increase in growing season length between 11–17 days per decade.

3.4.4. Agroecosystem level trends of rainfall onset date, cessation date and length of growing period

Results of AES level trend analysis of onset and cessation date, and growing season length revealed that only AES_3 and AES_5 had a significant trend in rainfall onset date, where the onset date decreased by 0.5 and 5.9 days per decade, respectively (Table 8).

The remaining AESs showed insignificant decreasing trends in rainfall onset date. Both cessation date and growing season length showed insignificant negative trends except for AES₃, which showed an insignificant increasing trend in growing season length (Table 8).

4. Discussion

Results of the present analysis showed that the rainfall onset date appears between the middle of the second week of May and the end of the second week of June in the entire area of the Choke Mountain watersheds. Areas in AES₃.AES₅ had particularly early rainfall onset date. These areas are known for maize (AES₃ and AES₄) and potato (AES₄ and AES₅) production, where both crops are planted following rainfall onset. Therefore, the existing agricultural calendar should be revised to fulfill all the necessary prerequisites to synchronize planting date and rainfall

onset date. At AES level, AES_3 and AES_5 had a significant trend in the rainfall onset date indicating the presence of a seasonal change in rainfall onset that required revision of all agricultural calendars.

Rainfall onset date also showed interannual variability which poses a great burden to farmers' agricultural calendar. Survey participants confirmed that the inconsistency of rainfall onset date leads to impulsive decision making on crop choice, land preparation and related activities, and that variability in onset date is a major factor affecting year-to-year changes in productivity and food security. This farmer perception is confirmed by the analysis of long-term observed climate records, in which 36-85% of the years included in the study period experienced false starts in the main rainy season. Surprisingly, a difference of up to 78 days has been found in rain onset date between the farmers' definition and optimal start date, and high elevation AESs (AES₄ and AES₅) showed the widest gaps. Farmers in these areas sow potato and maize by assuming that rain will continue in a reliable way once it starts. However, long dry spells following short rain showers have a significant negative effect on crop growth and subsequent yield. More than 80% of the years in the study period have more than four weeks dry spell length in February and March and planting in these months is the riskiest decision. Only farmers with access to supplementary irrigation supplies can plant in these months on account of this risk. Planting at the beginning of April is also risky as most of the years experienced a dry spell length of more than three weeks unless supplementary irrigation is considered.

The late rain start date in the eastern part of the study region (Fig. 2a) and generally earlier cessation in the south than in the north (Fig. 2b) resulted in shorter growing season length in the southeastern part of the study area (Fig. 2c), It should be noted, however, that these areas are dominated by vertisols with high water holding capacity, such that

Table 8Trends of onset, cessation, and growing season length in the study areas (1981–2016).

AES	Onset date (Onset date (DoY)			Cessation date (Doy)			Growing season length (days)		
	Mean	ZMK	Slope	Mean	ZMK	Slope	Mean	ZMK	Slope	
1	155	-0.55	-0.12	283	-1.21	-0.19	128	-0.15	-0.03	
2	169	-0.28	-0.29	303	-1.25	-0.21	134	-0.52	-0.17	
3	153	-1.83	-0.50	302	-0.16	-0.02	149	1.46	0.54	
4	159	-1.28	-0.35	306	-1.20	-0.18	147	0.53	0.28	
5	154	-1.93	-0.59	304	-1.23	-0.29	149	1.25	0.35	

AES= Agroecosystem, DoY = Day of the year (Julian date), ZMK = Mann Kendal trend test, Bold slope values indicate significant trend.

residual soil moisture can be retained well beyond the cessation of rains.

Trend tests revealed that onset date in AES_3 and AES_5 showed a significant decreasing trend (early onset). At site level, 31%, 25%, and 17% of the sites showed a significant decreasing trend in OD, CD, and LGP, respectively. Only 6% of the sites showed a significant increasing trend in LGP. The decreasing trend in OD calls for careful evaluation of the agricultural calendars, and the types of major crops/varieties grown in the area. For instance, for sites that showed significant decreasing trend in dry lower AESs, early maturing varieties of sorghum and maize should be considered to avoid any potential terminal drought damage on currently growing late maturing crop varieties such as BH-660 and BH-661 of maize (Amdu et al., 2013).

Cessation date and LGP do show significant positive correlations with elevation, indicating that higher elevation AESs have later rain cessation dates and longer growing periods. However, these results showed that the historical results may not apply prospectively, and forecasting services are critically important to provide evidence-based information for farmers for better decision making. From the survey, it was found that farmers face a critical challenge in defining the onset of rain and associated farm practices. They emphasized that getting tailor-made prior information for the coming season rain could boost farm productivity. Previous studies in the area also highlighted the importance of climate information. Amdu et al. (2013) performed a model-based study in the study area and reported that climate information had a positive contribution for climate change adaptation.

Implementing forecasting services may require resources, technology, data, and expertise that make them untenable for specific sites. However, the strong positive correlation among AESs for onset dates suggests that a service established for the Choke Mountain area in general may be applicable across AES, except for AES $_2$ that has a significant difference in OD variability from other AESs. However, the difference in AES $_2$ is just an offset then AES $_2$ could be addressed by a general forecast system.

The strong correlation between onset date and growing season length is also an indicator that early season information can usefully inform farm activities. Decision makers can make reasonably accurate estimates of growing season length based on rain onset date, such that a reliable forecast of onset date could be used as a forecast of the growing season. The need for a forecast system that can reliably predict the cropoptimal rainfall onset date—i.e., the onset date that accounts for the risk of a false start—is particularly critical given the large discrepancies found between onset date based on a traditional farmers' definition and that of a crop-optimal onset date to inform planting.

Survey results in AES4 and AES5 showed that potato sowing date is between February 26 and March 30, as late planting exposes the crop to late blight disease (Phytophthora infestans) before it attains its maturity stage (Supplementary Table 1). The statistical analysis revealed that both months (February and March) had very long dry period with a significant increasing trend in these AESs. Long dry spells and trends towards a delayed onset date are found, which greatly affect the production of potato, and pose a significant risk for early planting. Since a delayed potato crop can prevent double cropping in these areas, this will exacerbate food insecurity problem in the area. Early planting of potato is also advantageous for farmers as they get a chance to sow a second crop after potato harvesting in June-July. Thus, a seasonal shift in rains that delays potato planting will affect the food security of the already food insecure area (Ademe et al., 2020; Simane et al., 2016). Generally, access to different potato varieties, promotion of alternative cropping systems, and/or increased access to irrigation could be necessary to counteract this trend.

5. Conclusion

The present analysis indicated that onset dates, cessation dates, and growing season lengths showed high interannual variability across agroecosystems of Choke Mountain. The results also showed significant

false starts and dry spell risks which lead to frequent replanting and crop loss in the area. Despite the trend is different from specific sites grouped in each AES, some AESs also showed a significant trend change in onset date that points to the need to revise the recommended crop production calendar in the area. It should be noticed that site-specific results are complicated to provide actionable information for decision makers since contrasting results are found within the same AES. AES level analysis can provide plausible results which could be applicable for better decision making to minimize the impacts of crop failure.

Objective statistical analyses is generally consistent with farmers perceptions, and farmers generally perceive that rain onset date is highly variable, and they indicated that unpredictability of rainfall timing affects their choice of crop management practices. For this reason, they stressed the need tailored information on rain onset date to enable better crop decision making. Thus, establishing forecasting services should be a priority in the agricultural sector to provide actionable estimates of onset and general rainfall pattern for the coming season. In areas (AES₄ and AES₅) where potato is a main crop different and integrated management practices; access to resistant varieties, use of alternative crops and increased access to irrigation could be necessary to adapt the ill effects of long dry spells.

Declaration of Competing Interest

The authors declare that they have no known competing financial interests or personal relationships that could have appeared to influence the work reported in this paper.

Acknowledgments

The first author was supported by the Belmont Forum Collaborative Research (NILE-NEXUS- a project award number 1624335) funded by the National Science foundation (NSF). The authors wish to acknowledge the Ethiopian National Meteorological Services Agency (NMA) for providing data used in this study. The CCl/WCRP/JCOMM Expert Team on Climate Change Detection and Indices (ETCCDI) is also acknowledged for the provision of access to the RHtestsV3 and RHtests_dlyPrcp software packages used for homogeneity test and change point detection and for their technical comments. Department of Earth and Planetary Sciences, Johns Hopkins University is also acknowledged for hosting the first author as a visiting student.

Supplementary materials

Supplementary material associated with this article can be found, in the online version, at doi:10.1016/j.agrformet.2021.108697.

References

Ademe, D., Ziatchik, B.F., Tesfaye, K., Simane, B., Alemayehu, G., Adgo, E., 2020. Climate trends and variability at adaptation scale: patterns and perceptions in an agricultural region of the Ethiopian Highlands. Weather Clim. Extrem. 29, 100263 https://doi.org/10.1016/j.wace.2020.100263.

Aguilar, C., Polo, M.J., Dynamics, F., 2011. Generating reference evapotranspiration surfaces from the Hargreaves equation at watershed scale. Hydrol. Earth Sci. Syst. 15, 2495–2508. https://doi.org/10.5194/hess-15-2495-2011.

Akinseye, F.M., Agele, S.O., Traore, P.C.S., Adam, M., Whitbread, A.M., 2016. Evaluation of the onset and length of growing season to define planting date—'a case study for Mali (West Africa). Theor. Appl. Climatol 124, 973–983. https://doi.org/10.1007/s00704-015-1460-8.

Alemayehu, A., Bewket, W., 2017. Local spatiotemporal variability and trends in rainfall and temperature in the central highlands of Ethiopia. Geogr. Ann. Ser. A Phys. Geogr. 99, 85–101. https://doi.org/10.1080/04353676.2017.1289460.

Amarasingha, R.P.R.K., Galagedara, L.W., Marambe, B., Silva, G.L.L.P.,

Amarasingha, R.P.R.K., Galagedara, L.W., Marambe, B., Silva, G.L.L.P., Punyawardena, R., Nidumolu, U., Howden, M., Suriyagoda, L.D.B., 2015. Aligning sowing dates with the onset of rains to improve rice yields and water productivity: modelling rice (Oryza sativa L.) yield of the Maha season in the dry zone of Sri Lanka. Trop. Agric. Res. 25 (277) https://doi.org/10.4038/tar.v25i3.8038.

Amdu, B.A., Ayehu, A., Deressa, A., 2013. Farmers' Perception and Adaptive Capacity to Climate Change and Variability in the Upper Catchment of Blue Nile, Ethiopia

- Farmers' Perception and Adaptive Capacity to Climate Change and Variability in the Upper Catchment of Blue Nile, Ethiopia.
- Aramde, F., Demelash, A., Yosef, Mm., 2014. Effects of landuse and land cover changes on the extent and distribution of afroalpine vegetation of Northern Western Ethiopia: the case of Choke Mountains. Res. J. Environ. Sci. 8, 17–28. https://doi.org/ 10.3923/rjes.2014.17.28.
- Assefa, Y., Staggenborg, S.A., Prasad, V.P. V., 2010. Grain Sorghum Water Requirement and Responses to Drought Stress: A Review. Cm 9, 0. doi:10.1094/cm-2010-1109-01
- Basu, S., Ramegowda, V., Kumar, A., Pereira, A., 2016. Plant adaptation to drought stress [version 1; referees: 3 approved]. F1000Research 5, 1–10. https://doi.org/
- Berhane, F., Zaitchik, B., Dezfuli, A., 2014. Subseasonal analysis of precipitation variability in the Blue Nile River Basin. J. Clim. 27, 325–344. https://doi.org/ 10.1175/JCLI-D-13-00094.1.
- Brewbaker, J.L., 2003. Corn Production in the Tropics The Hawaii Experience. College of Tropical Agriculture and Human Resources. University of Hawaii at Manoa.
- Dinku, T., Cousin, R., Corral, J., Ceccato, P., Thomson, M.C., Faniriantsoa, R., Khomyakov, I., Vadillo, A., 2016. The ENACTS Approach: transforming climate services in Africa one country at a time. World Policy Pap 1–24.
- Dinku, T., Hailemariam, K., Maidment, R., Tarnavsky, E., Connor, S., 2014. Combined use of satellite estimates and rain gauge observations to generate high-quality historical rainfall time series over Ethiopia. Int. J. Climatol. 34, 2489–2504. https:// doi.org/10.1002/joc.3855.
- Eggen, M., Ozdogan, M., Zaitchik, B., Ademe, D., Foltz, J., Simane, B., 2019.
 Vulnerability of sorghum production to extreme, sub-seasonal weather under climate change. Environ. Res. Lett. 14, 045005 https://doi.org/10.1088/1748-9326/aafe19.
- Funk, C., Peterson, P., Landsfeld, M., Pedreros, D., Verdin, J., Shukla, S., Husak, G., Rowland, J., Harrison, L., Hoell, A., Michaelsen, J., 2015. The climate hazards infrared precipitation with stations - a new environmental record for monitoring extremes. Sci. Data 2, 1–21. https://doi.org/10.1038/sdata.2015.66.
- Gbangou, T., Ludwig, F., van Slobbe, E., Hoang, L., Kranjac-Berisavljevic, Gordana, 2019. Seasonal variability and predictability of agro-meteorological indices: tailoring onset of rainy season estimation to meet farmers' needs in Ghana. Clim. Serv. 14, 19–30. https://doi.org/10.1016/j.cliser.2019.04.002.
- Gelaro, R., McCarty, W., Suárez, M.J., Todling, R., Molod, A., Takacs, L., Randles, C.A., Darmenov, A., Bosilovich, M.G., Reichle, R., Wargan, K., Coy, L., Cullather, R., Draper, C., Akella, S., Buchard, V., Conaty, A., da Silva, A.M., Gu, W., Kim, G.K., Koster, R., Lucchesi, R., Merkova, D., Nielsen, J.E., Partyka, G., Pawson, S., Putman, W., Rienecker, M., Schubert, S.D., Sienkiewicz, M., Zhao, B., 2017. The modern-era retrospective analysis for research and applications, version 2 (MERRA-2). J. Clim. 30, 5419–5454. https://doi.org/10.1175/JCLI-D-16-0758.1.
- Gessesse, A.A., Melesse, A.M., 2018. Decadal dynamics of land use/land cover in the Muga Watershed, Choke Mountain Range. Upper Blue Nile Basin 1–13. https://doi. org/10.20944/preprints201805.0262.v1.
- Gilbert, R.O., 1987. Statistical methods for environmental pollution monitoring. VNR, New York.
- Gocic, M., Trajkovic, S., 2013. Analysis of changes in meteorological variables using Mann-Kendall and Sen's slope estimator statistical tests in Serbia. Glob. Planet. Change 100, 172–182. https://doi.org/10.1016/j.gloplacha.2012.10.014.
- Gotardo, J.T., Rodrigues, L.N., Gomes, B.M., 2016. Comparison of methods for estimating reference evapotranspiration: an approach to the management of water resources within an experimental basin in the brazilian cerrado. Eng. Agric. 36, 1016–1026. https://doi.org/10.1590/1809-4430-Eng.Agric.v36n6p1016-1026/ 2016
- IRI, 2016. Why ENACTS ? A training module, version 1. International Research Institute for Climate and Society.
- Karl, T.R., Nicholls, N., A.G., 1999. Clivar/GCOS/WMO workshop on indices and indicators for climate extremes workshop summary. Clim. Chang. 42, 3–7.
- Limantol, A.M., Keith, B.E., Azabre, B.A., Lennartz, B., 2016. Farmers' perception and adaptation practice to climate variability and change: a case study of the Vea catchment in Ghana. Springerplus 5. https://doi.org/10.1186/s40064-016-2433-9.

- Mann, H.B., 1945. Nonparametric Tests Against Trend Author (s): Henry B . Mann Published by. The Econometric Society Stable, pp. 245–259. URL: https://www.jstor.org/stable/1907187 REFERENCES Linked references are available on JSTOR for this article: You may need to log in to JSTOR 13.
- Mellander, P.E., Gebrehiwot, S.G., Gärdenäs, A.I., Bewket, W., Bishop, K., 2013. Summer rains and dry seasons in the upper blue nile basin: the predictability of half a century of past and future spatiotemporal patterns. PLoS One 8, 1–12. https://doi.org/10.1371/journal.pone.0068461.
- Ratan, R., Venugopal, V., 2013. Wet and dry spell characteristics of global tropical rainfall. Water Resour. Res. 49, 3830–3841. https://doi.org/10.1002/wrcr.20275.
- Sarr, B., 2012. Present and future climate change in the semi-arid region of West Africa: a crucial input for practical adaptation in. Atmos. Sci. Lett. 13, 108–112. https://doi. org/10.1002/asl.368.
- Saxton, K.E., Rawls, W.J., Romberger, J.S., R.I.P., 1986. Estimating soil water characteristics-hydraulic conductivity. Soil Sci. Soc. Am. J. 5, 1031–1036.
- Selvaraju, R., 2011. Climate risk assessment and management in agriculture. Build. Resil. Adapt. to Clim. Chang. Agric. Sect. 23, 71–90. https://doi.org/10.1103/ PhysRevD.64.104020 https://doi.org/doi:
- Sen, P.K., 1968. Estimates of the Regression Coefficient Based on Kendall 's. Tau. J. Am. Stat. Assoc. 63, 1379–1389.
- Simane, B., Zaitchik, B.F., Foltz, J.D., 2016. Agroecosystem specific climate vulnerability analysis: application of the livelihood vulnerability index to a tropical highland region. Mitig. Adapt. Strateg. Glob. Chang. 21, 39–65. https://doi.org/10.1007/ s11027-014-9568-1
- Simane, B., Zaitchik, B.F., Mesfin, D., 2012. Building climate resilience in the Blue Nile/ Abay Highlands: a framework for action. Int. J. Environ. Res. Public Health 9, 610–631. https://doi.org/10.3390/ijerph9020610.
- Simane, B., Zaitchik, B.F., Ozdogan, M., 2013. Agroecosystem analysis of the choke mountain watersheds. Ethiopia. Sustain. 5, 592–616. https://doi.org/10.3390/ su5020592.
- Stern, R.D., Dennett, M.D., Garbutt, D.J., 1981. The start of the rains in West Africa. J. Climatol. 1, 59–68.
- Stern, R, Rijks, D., Dale, I., Knock, J., 2006. INSTAT climatic guide. Stat. Serv. Centre, Univ. Reading.
- Suryabhagavan, K.V., 2017. GIS-based climate variability and drought characterization in Ethiopia over three decades. Weather Clim. Extrem. 15, 11–23. https://doi.org/ 10.1016/j.wace.2016.11.005.
- Teegavarapu, R.S.V., Chandramouli, V., 2005. Improved weighting methods, deterministic and stochastic data-driven models for estimation of missing precipitation records. J. Hydrol. 312, 191–206. https://doi.org/10.1016/j. ihydrol.2005.02.015.
- Teferi, E., Uhlenbrook, S., Bewket, W., Wenninger, J., Simane, B., 2010. The use of remote sensing to quantify wetland loss in the Choke Mountain range, Upper Blue Nile basin. Ethiopia. Hydrol. Earth Syst. Sci. 14, 2415–2428. https://doi.org/ 10.5194/hess-14-2415-2010.
- Urgessa, T.B., 2014. Review of challenges and prospects of agricultural production and productivity in Ethiopia. J. Nat. Sci. Res. 4, 70–77.
- Viste, E., Korecha, D., Sorteberg, A., 2013. Recent drought and precipitation tendencies in Ethiopia. Theor. Appl. Climatol. 112, 535–551. https://doi.org/10.1007/s00704-012-0746-3.
- Wang, X.L., 2008a. Penalized maximal F test for detecting undocumented mean shift without trend change. J. Atmos. Ocean. Technol. 25, 368–384. https://doi.org/ 10.1175/2007JTECHA982.1.
- Wang, X.L., 2008b. Accounting for autocorrelation in detecting mean shifts in climate data series using the penalized maximal t or F test. J. Appl. Meteorol. Climatol. 47, 2423–2444. https://doi.org/10.1175/2008JAMC1741.1.
- Weldlul, A., 2016. Analysis of smallholder farmers' perceptions of climate change and adaptation strategies to climate change: the case of Western Amhara Region, Ethiopia.
- Zaitchik, B.F., Simane, B., Habib, S., Anderson, M.C., Ozdogan, M., Foltz, J.D., 2012. Building climate resilience in the Blue Nile/Abay Highlands: a role for earth system sciences. Int. J. Environ. Res. Public Health 9, 435–461. https://doi.org/10.3390/ijerph9020435.